Field Identification of Weed Species and Glyphosate-Resistant Weeds Based on UAS Imagery in Early Growing Season

Alimohammad Shirzadifar, Sreekala Bajwa, John Nowatzki, Aliasghar Bazrafkan

Shirzadifar, A., Bajwa, S., Nowatzki, J., & Bazrafkan, A. (2020). Field identification of weed species and glyphosate-resistant weeds using high resolution imagery in early growing season. Biosystems Engineering, 200, 200-214

https://doi.org/10.1016/j.biosystemseng.2020.10.001

Field Identification of Weed Species and Glyphosate-Resistant Weeds Based on UAS Imagery in Early Growing Season

Alimohammad Shirzadifar[1*], Sreekala Bajwa[2], John Nowatzki[1], Aliasghar Bazrafkan[3]

[1] Department of Agricultural & Biosystems Engineering, North Dakota State University, Fargo, ND, USA.

[2] Montana State University, Bozeman, MT, USA.

[3] Agriculture and Natural Resource Department, Yazd university, Yazd, Iran.

* Corresponding author: Alimohammad Shirzadifar

Email address: Alimohammad.shirzadi@ndsu.edu

Tel.: +17017997759

ORCID: 0000-0002-2547-0397

Abstract

Accurate weed mapping in early growing season is an essential step in the site-specific weed management (SSWM) system. This study focuses on validating the potential application of high resolution multispectral and thermal UAS images in classification of weed species and glyphosate-resistant weeds at early phenological stages. A field experiment was conducted to evaluate supervised classification methods to identify three-weed species including waterhemp, kochia, and ragweed. The accuracy of six classification algorithms namely Parallelepipeds (P), Mahalanobis Distance (MD), Maximum Likelihood (ML), Spectral Angle Mapper (SAM), Support Vector Machine (SVM) and Decision Tree (DT) implemented at pixel and object- based in weed species classification were evaluated. Thermal infrared imagery was also used to assess the canopy temperature variance within the weed species to identify the glyphosate- resistance status in detected weeds. The object-based algorithms developed with mosaicked imagery effectively classified weed species with the overall accuracy and Kappa coefficient values greater than 86% and 0.77, respectively. The lowest accuracy and Kappa coefficient (67% and 0.58) were

observed for pixel-based MD algorithm. The canopy temperature-based classification of susceptible and resistant weeds resulted in the discrimination accuracies of 88%, 93% and 92% in glyphosate-resistant kochia, waterhemp and ragweed, respectively.

Keywords: Weed species; Glyphosate-resistant weeds; UAS imagery; Object-based classification.

1. Introduction

Weeds are considered as the most serious threat to agricultural crops as they compete with crops for water, nutrients, and light, resulting in yield reduction. Currently, herbicide application is the most common weed management technology in the US (Benbrook, 2018), where weed control is achieved through a uniform herbicide application across the entire field (Kunz, Weber, Peteinatos, Sökefeld, & Gerhards, 2018). However, weed species and populations across the field are highly variable (Lambert, Hicks, Childs, & Freckleton, 2018). Chemical weed management is of great interest owing to increased concern over environmental protection as well as the emergence of herbicide resistant weeds as a result of sub-optimal application of chemicals (Schütte et al., 2017).

In the context of precision agriculture, site-specific weed management (SSWM) is an emerging strategy, confining the application of herbicides to weed infested areas to improve crop protection efficacy (Pflanz, Nordmeyer, & Schirrmann, 2018). The SSWM strategy includes four steps of weed monitoring, decision making, herbicide application, and evaluation and documentation. Weed mapping as the first step is a key element in SSWM, collecting data for field survey and weed distribution either by ground sampling or remote detection. Remote sensing that captures the whole field offers particular advantages for weed mapping over traditional ground survey methods including large area coverage, facile data collection, and time-efficient process (Gålfalk, Karlson, Crill, Bousquet, & Bastviken, 2018).

The recent advances in Unmanned Aerial System (UAS) facilitate the application of time-efficient field mapping in large scale in modern agriculture. Small UAS with light weight and high level of maneuverability are capable of carrying different sensors and flying at low altitude over agricultural fields (Sosnowski, Bieszczad, Madura, & Kastek, 2018). Very high ground resolution (pixel<5cm) UAS images can be used to identify and map the spatial distribution of weeds within crop fields when spectral differences among weeds, crop and soil are present and quantifiable

(Castillejo-González, Pena-Barragán, Jurado-Expósito, Mesas-Carrascosa, & López-Granados, 2014). Although, Garcia-Ruiz et al. (2013) used low attitude UAS equipped with multi spectral camera to detect different plants, traditional pixel-based image analysis cannot effectively detect weeds in crop fields during early growth stages due to spectral similarity of crop and weed pixels, and the variability in spectral characteristics of similar plants caused by field variability.

The application of supervised classification methods using ground-based imaging devices has shown promise in weed classification (Pérez-Ortiz et al., 2015). Remote sensing based high-resolution UAS imagery in combination with supervised classification holds the potential to identify weed species. Supervised pixel-based classifiers use prior knowledge to identify spectral similarity in image pixels to assign each pixel to the most similar class. Supervised classification methods include the simplest distance- or angular-based classifiers (Mahalanobis Distance and Spectral Angel Mapper) to the most complex probability-based (maximum likelihood) or machine learning (support vector machine and decision tree) algorithms. Each classifier has its own strengths and limitations, and the selection of a classifier for specific site study requires the consideration of many factors, including data distribution, classification accuracy, algorithm performance, and computational resources.

In UAS-based remote sensing, object-based image analysis (OBIA) and pixel-based image analysis (PBIA) are two categories of image classification. In conventional PBIA supervised weed classification, each pixel could potentially include a mixture of soil, plant leaves, residue and shadow. The variability in target spectral reflectance introduced by mixing of target classes can limit the classification accuracy. In contrast, the geographic OBIA recognizes spatially and spectrally homogenous objects through a segmentation process based on different attributes, such as size, texture, shape, spatial and spectral distribution (Liu & Abd-Elrahman, 2018). These factors can be combined with contextual and hierarchy procedures to give an accurate classification in OBIA (Pena, Torres-Sánchez, de Castro, Kelly, & López-Granados, 2013). A comparative study on the performances of PBIA and OBIA to discriminate weeds and sorghum plant indicated higher accuracy for OBIA (Che'Ya (2016).

The visual similarity between herbicide-resistant and susceptible weeds limits the identification accuracy of herbicide resistance status. Accordingly, SSWM may not be effectively accomplished using the application of common visual plant species identification techniques. Therefore, the application of different methods capable of providing higher accuracy in identification is needed. It was reported that the application of herbicide can cause stress in plants and this, in turn, can reduce the rates of photosynthesis and transpiration in the plants. Reduced transpiration rate is accompanied by elevated temperatures in stressed plants (Zhang, Filella, Garbulsky, & Peñuelas, 2016). Therefore, we hypothesized that the canopy temperature after spraying can be a reliable indicator to detect resistant weeds.

This research aims at exploring the potential of multispectral imagery captured by UAS over crop fields for weed species identification, followed by the application of thermal images for the identification of herbicide resistant weeds. Field experiment was conducted with the objective of identifying and validating the best PBIA and OBIA supervised classification methods to identify three weed species including waterhemp (*Amaranthus rudis*), kochia (*Kochia scoparia*), and ragweed (*Ambrosia artemisiifolia L.*). The detected weeds were then classified into glyphosate resistant and susceptible categories by the application of canopy temperature after an herbicide application.

2. Materials and Methods

2.1. Study Site and Field Experiment Design

A field-scale study was conducted on a 680 m^2 soybean crop field at NDSU Research Farm located at Carrington, North Dakota, USA (Figure 1). The Roundup Ready NuTech Soybean (Glycine max) was planted on May 22nd, 2017 at 403845 seeds/ha. For field experiment, two common types of weeds (kochia and waterhemp) were grown in the greenhouse in separate pots, and the pots were transferred into the field at 5-7 leaf stage (Figure 2). The weed plants were transplanted randomly in the fields to create a mix of main crop and weed species. The seeds for the weeds were collected randomly from different parent plants to provide a collection of resistant and susceptible plants.

Field data were also collected from a 400 m^2 research field located at Mayville (Figure 1). The field was naturally infested with glyphosate-resistant and susceptible lambsquarters, and ragweed (Figure 2). Weeds on the fields were manually identified and tagged with their species and geographic coordinates through field scouting. When the weeds were approximately 7.6 cm tall, glyphosate [N-(phosphonomethyl) glycine] of 1.7% concentration was applied to the fields at a uniform rate.

Figure 1. Field sites: a) Google Maps® inset showing the general location of the study sites with blown up views of fields at b) Carrington, c) Mayville.

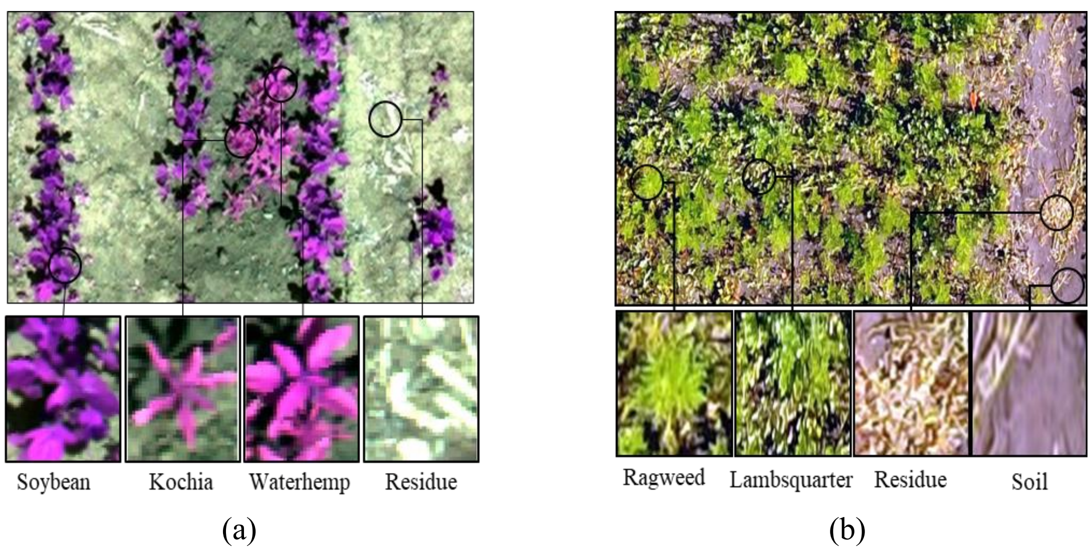

Figure 2. A multispectral image illustrating the target classes in the two study sites: a) Carrington (false color image), b) Mayville (RGB image).

2.2. Data Collection

The aerial data acquisition system was composed of a multispectral camera (Quad sensor, Sentera, Minnesota, USA) and a thermal camera (Infrared Camera Inc. Texas, USA), mounted separately on two small UASs. Two Quadcopters namely Phantom3 and DJI S1000 (SZ, DJI Technology Co., Ltd., Shenzhen, China) were used to fly the cameras over the experimental fields for collecting multispectral and thermal images, respectively (Table 1). Multispectral images were used to classify weed species. Thermal images were captured 4 days after glyphosate application and were used to identify herbicide resistance status in the weeds. Direct georeferencing of acquired images with the accuracy of 20 centimeter was provided by dual on-board navigation-grade GPS and GLONASS receiver.

Table 1. Summary of cameras and flight procedures in the study.

Item	Camera type	
	Multispectral	Thermal
UAS	Phontom3	S1000
Sensor name	Sentera Quad	9640 P-Series USB
Sensor type	CMOS	UFPA (VO×)
Max-pixels	10.5 MP RGB, 3×1.2MP	640×480
Length of focus	6.05 mm	25mm
Sensor size	56×96×52 mm	34×30×34 mm
Channels	RGB,670,710,730	7µm-14µm
Average wind speed	4.5 m/s	3.2 m/s
Average altitude	10.1 m	8 m
Average pixel size on the ground	6.14 mm	5.5 mm
Forward overlap	60	65
Side overlap	70	80
FOV[a]	44° H	24.8 × 18.6

UAS images were captured at low flying altitudes of 8 m for thermal, and 10.1 m for multispectral. The area covered by each single image was limited. The still images collected from UAS at 60-65% forward overlap, and 70-80% side overlap were mosaicked to obtain an image covering the whole study area. In total, 750 multispectral images were recorded for the soybean farms at NDSU Research Center and 420 multispectral images were captured over the study field located at Mayville.

Five ground control points including four points at the field corners and a coordinate close to the field center point were marked for bundle block adjusting. The flight route was programmed using DJI GS PRO app to allow the UAS to acquire data automatically at pre-set waypoints. In addition, the flight altitude and required image overlapping for mosaicking process was also managed using DJI GS PRO app.

2.3. Image Calibration

During data collection, a standard spectralon split gray level panel reference (Labsphere Inc., North Sutton, NH, USA) was placed in the middle of the field to calibrate spectral data. Digital images captured by multispectral camera were spectrally corrected by applying an empirical linear calibration method (Hunt et al., 2010). The mean values of three bands (blue, green, and red) in an image before and after correction is shown in Figure 3.

2.4. Image Mosaicking

Prior to implementing image processing steps to identify weeds, the individual images were mosaicked to create a single image representing the whole field. Agisoft Photoscan Professional Edition (Agisoft LLC, St. Petersburg, Russia) software was employed to orthorectify and mosaic the collected images. A point cloud model was developed by finding the geographical position and principal axes (roll, pitch and yaw) of the camera in each acquired image and aligning the images automatically with the Agisoft Photoscan software. Then, the individual images were projected over a geometry of 3D construction to generate an orthophoto map. The final step was developing a single image representing the whole study site.

(a)

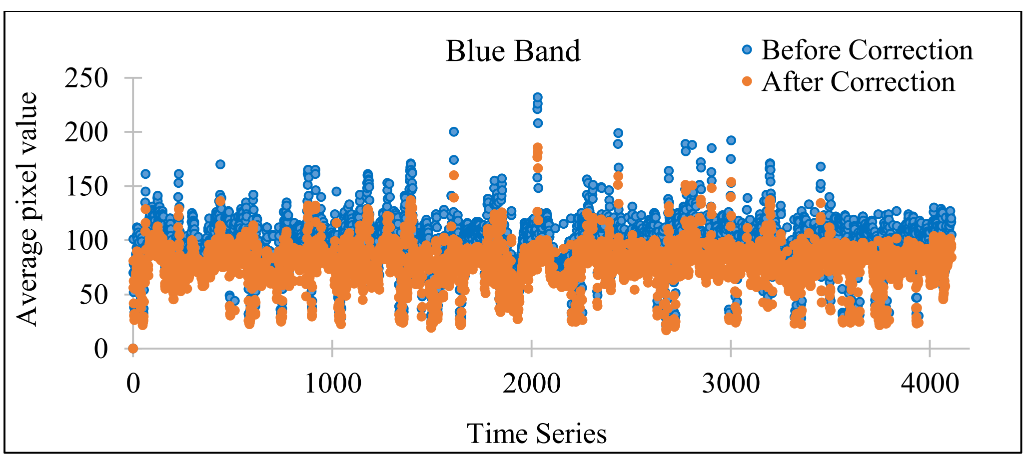

(b)

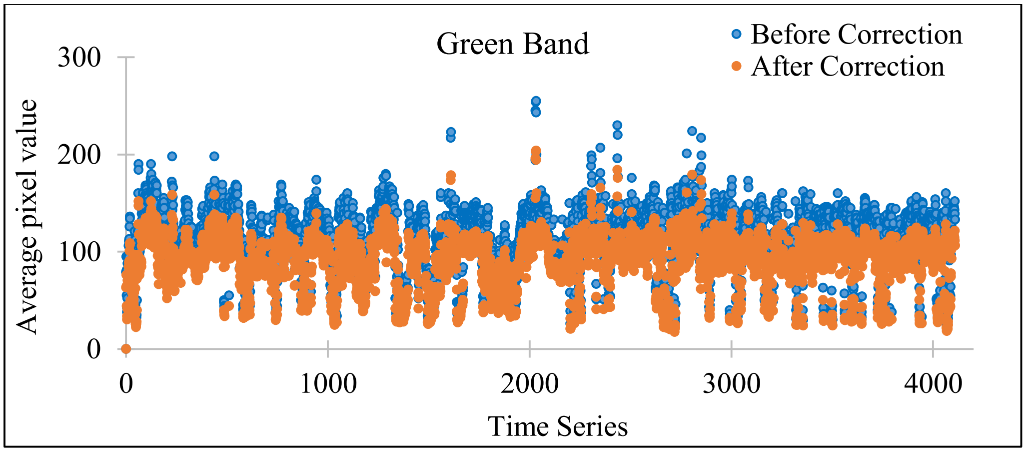

(c)

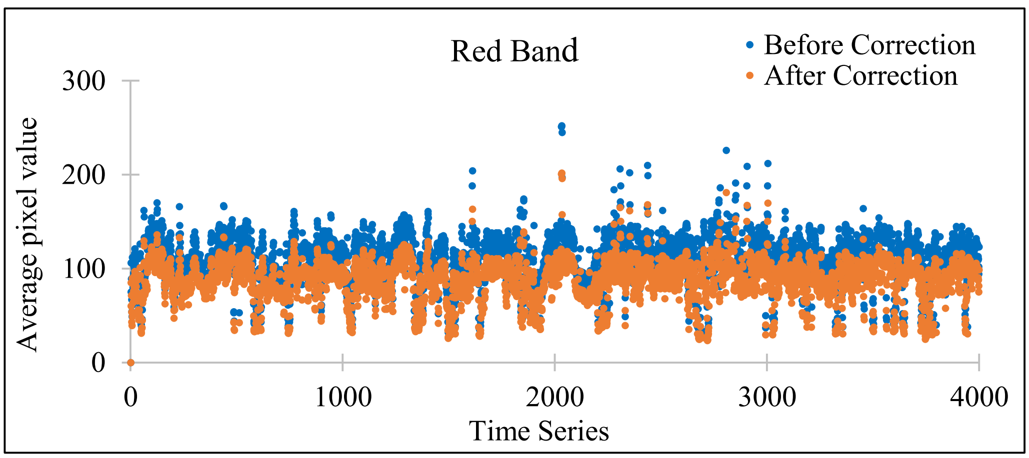

Figure 3. Calibrating RGB band Digital Numbers (DNs), in an empirical line correction approach. a) Blue band, b) Green band, c) Red band.

2.5. Spectral Separability Analysis

The application of supervised classification methods on large image sets is time and effort-intensive. To identify the best method, the feasibility of classifications algorithms in field target class detection was evaluated based on visual differences in spectral signature, principal component analysis (PCA), and scatter plots of spectral reflectance. Spectral signature of plant species, bare soil and residue were developed using spectral reflectance at four bands including RGB, 670, 710, and 730 nm. The PCA is a statistical method that uses orthogonal transformation to transform a set of observations of possibly correlated variables into a set of values of linearly uncorrelated variables called principal components (Voyant et al., 2017). Due to the high degree of spatial similarity between spectral signatures, PCA is used to identify the most significant variance in the spectral reflectance of target classes. The scatter plot of target spectral reflectance in the first two PC space can illustrate the separability of target classes.

2.6. Segmentation Procedure

Segmentation is a key factor in OBIA classification methods. The captured images were segmented using a multi-resolution algorithm to create homogeneous multi-pixel objects corresponding to crop, weed species, bare soil and residue. The multi-resolution segmentation method minimizes the average heterogeneity and produces highly homogeneous image objects at an arbitrary resolution. The image objects were generated from the spectrally and spatially similar pixels based on a set of input parameters including shape, smoothness, compactness, etc (Table 2). The OBIA method designed for weed mapping objectives was developed using the commercial software eCognition Developer 8.9 (Trimble GeoSpatial, Munich, Germany).

Table 2. The input information used for segmenting field images into objects for object-based classification.

Target	Compactness	Smoothness	Shape index	Roundness	Asymmetry	Elliptic fit	Density	Border index
Soybean	0.23	0.77	2.68	1.43	0.25	0.31	1.8	2.68
Waterhemp	0.5	0.5	1.4	0.75	0.69	0.54	2.31	1.25
Kochia	0.52	0.38	1.37	0.19	0.75	0.36	1.89	1.2
Ragweed	0.34	0.76	2.27	0.81	0.74	0.67	2.1	2.15
Lambsquarters	0.16	0.84	1.38	0.31	0.22	0.76	1.62	1.42
Residue	0.44	0.56	1.39	0.36	0.9	0.68	1.2	3.69

2.7. Image Classification

Weed species, crop and soil were classified using six supervised classification algorithms with both PBIA and OBIA methods. Six supervised classifiers with strong conceptual and mathematical differences including Parallelepiped (P), Maximum Likelihood (ML), Mahalanobis Distance (MD), Support Vector Machine (SVM), Spectral Angle Mapper (SAM), and Decision Tree (DT) were examined to select the optimum method for weed species classification (Castillejo-González et al., 2014). To evaluate the normality of UAS images data, the histogram graphical visual inspection with skewness and kurtosis parameters were used. Exploratory data analysis showed that image data were normally distributed and met the normality assumption for methods such as ML, MD and linear SVM.

The P classification method also known as the box decision rule, recognizes each class by defining square areas based on minimum and maximum reflectance values into spectral measures of training classes. The MD and SAM algorithms calculate the spectral distance and the spectral angle from each pixel to the spectral average of each class, respectively. The ML algorithm is a parametric supervised classifier based on the Bayes theorem and classifies the objects by considering the variance– covariance within the class distributions.

The SVM is a supervised learning algorithm that analyzes data as points in a feature space and identifies the pattern for classification. This model divides the data into separate categories by defining a clear gap between the categories as wide as possible. In this study, the linear SVM method was used due to obtaining more accurate result than non-linear functions. The DT is a predictive model that maps observations to their target values or labels. DT method makes classification rules by recursively partitioning the data into increasingly homogenous groups (Stephens & Diesing, 2014). In this study, the DT method was applied to the images using the C5 algorithm (Pandya & Pandya, 2015) that expands nodes in depth-first order in each step by the divide-and-conquer strategy. Mosaicked multispectral images were classified in ENVI 5.3 (Broomfield County, Colorado, US) software equipped with image processing toolbox.

The accuracy of each classification method was evaluated by developing the numerical confusion matrix (error matrix) and computing the kappa coefficient. The confusion matrix provides the overall accuracy of the classification by comparing the percentage of classified pixels of each class with the verified ground truth class. The Kappa coefficient is a measure of how the classification results compare to class labels assigned by chance. It can take values from 0 to 1, and the value of 0 indicates that there is no agreement between the classified image and the reference image. If kappa coefficient equals to 1, then the classified image and the ground truth image are totally identical.

2.8. Glyphosate-Resistant Weed Identification

After weed species identification step, herbicide resistance status was studied by comparing the canopy temperature 4 days after glyphosate application. Canopy temperature was obtained from thermal images using a 9640 P-Series Infrared Camera (ICI, Beaumont, TX, USA) with 7–14 μm spectral response and ±1°C accuracy. Thermal camera was mounted on DJI S1000 and images were processed using IR Flash software (Infrared Camera ICI. TX, USA) to identify glyphosate-resistant kochia and waterhemp in Carrington site, and resistant-ragweed in Mayville field. Before capturing the images, a Blackbody ICI 350 portable IR calibration (ICI. TX, USA) was used to check the camera calibration. Thermal images were captured in low altitude to develop high resolution (5.5 mm) images. Each individual thermal image covered a relatively small area of 1.6 m^2 in the field. In this study we assumed that the variations in thermal signature due to soil moisture content was negligible in a small field. Furthermore, atmospheric condition in each image was the same for both susceptible and resistant weeds (data were collected between 12 to 2 pm and the sky was clear) (Table 3). Therefore, the comparison of plant canopy temperature could lead to classify resistant versus susceptible weeds in each individual thermal image. Before starting the image capture, a Blackbody ICI 350 portable IR calibration (ICI. TX, USA) was used to check the camera calibration.

Table 3. Atmospheric conditions during the period of data collection in Carrington (S1) and Mayville (S2) study sites.

Study site	Data collection time	Air temperature (°C)	Relative humidity (%)
S1	12:15-12:30	32.13±0.01	48.32±0.00
S2	13:05-13:23	33.37±0.02	54.12±0.01

To identify glyphosate-resistant weeds based on canopy temperature, 16 thermal images captured form each field were analyzed separately by threshholding and segmentation in IR Flash software. The results were compared with the ground truth data to evaluate the accuracy, sensitivity, specificity, and precision through counting the false positives and the false negatives for herbicide resistance. Classifier performance was evaluated as two-class problems based on the confusion matrix. There are two classes namely positive and negative for herbicide resistance. Confusion matrix consists of true positive (TP), false positive (FP), false negative (FN) and true negative (TN) values. Since the objective of classification was to identify resistant weeds, the resistant weed (class R) was defined by a model output of positive and the susceptible weed (Class S) was defined by a model output of negative in this study. False positive represents the number of susceptible weeds which were identified as resistant. In contrast, false negative indicates the number of resistant weeds which were classified as susceptible ones. Accuracy was the ratio of correct decisions made by a classifier (Equation 1). Sensitivity and specificity were introduced to represent the proportion of actual resistant (Equation 2) or susceptible (Equation 3) species which are correctly classified, respectively. Precision was defined as the ratio of predicted positive examples which really were positive (Equation 4).

$$Accuracy = \frac{TP + TN}{TP + FP + FN + TN} \tag{1}$$

$$Sensitivity = \frac{TP}{TP + FN} \tag{2}$$

$$Specificity = \frac{TN}{TN + FP} \tag{3}$$

$$Precision = \frac{TP}{TP + FP} \tag{4}$$

The ground truth data were collected 15 days after glyphosate application to visually detect the resistant weeds. Glyphosate-resistant weeds on the field were identified and labeled with their geographic coordinates throughout the field.

An overview of weed species classification and identifying glyphosate-resistant weeds in this study is illustrated in Figure 4.

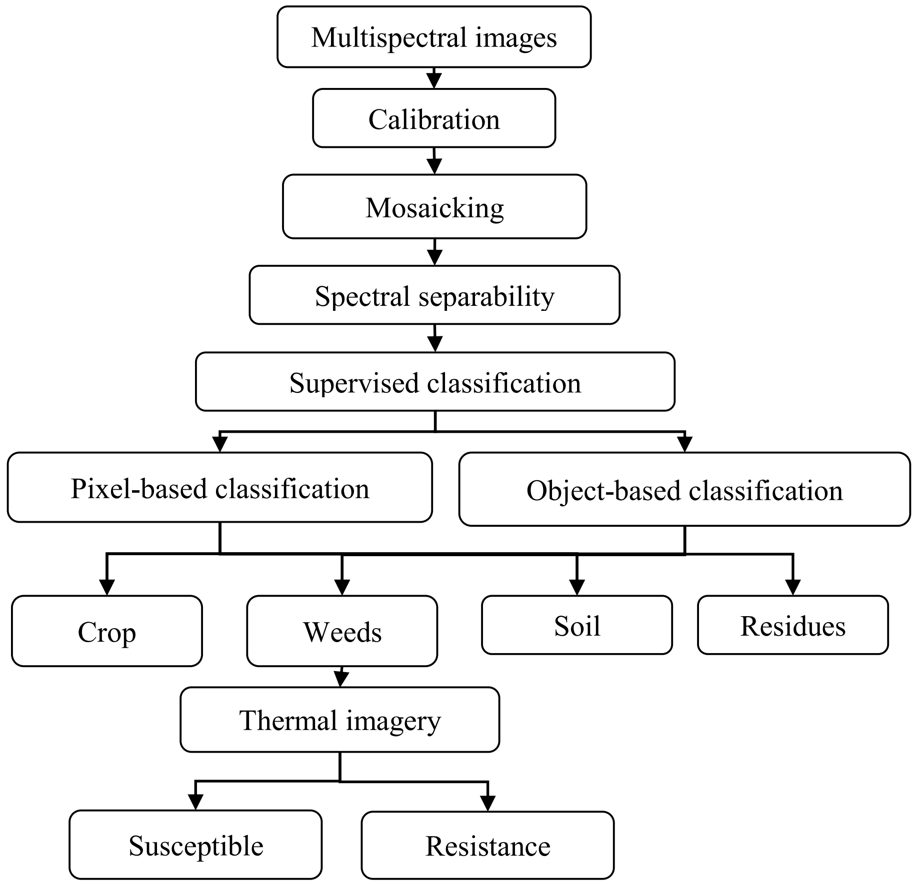

Figure 4. Flowchart of recognition algorithms applied for object classification and weed specious detection and glyphosate resistant weeds.

3. Results and Discussion

3.1. Spectral Reflectance Separability

The distinct spectral signatures for field components in both field studies are illustrated in Figures 5a and 5a. The scatter plot of spectral reflectance in the first two PC indicated that soybean and weed species in Carrington could be discriminated into separate classes considering spectral signature in red and blue wavebands (Figure 5).

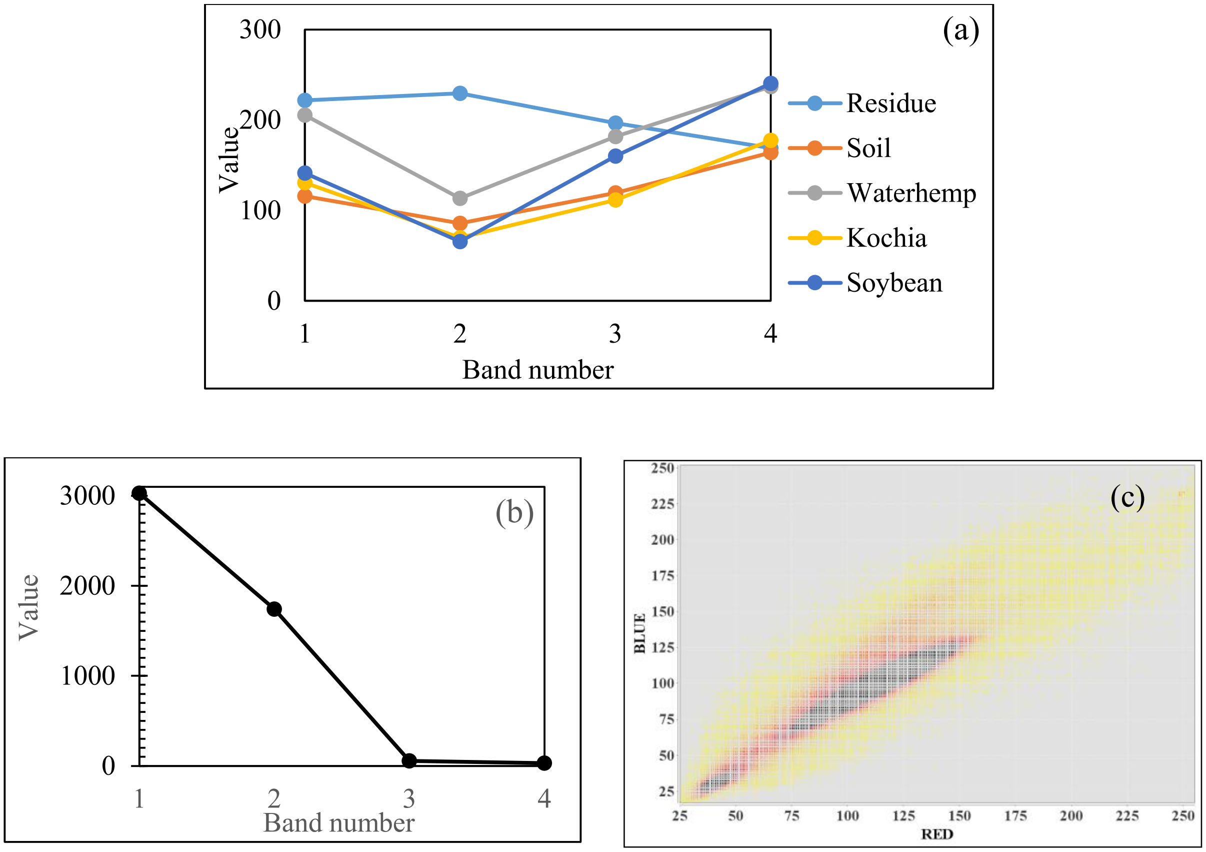

Figure 5. Assessment of feasibility of field components classification in Carrington study site: a) Spectral signature, b) PC plane, and c) Scatterplot of spectral reflectance. Band number 1 through 4 are RGB, 670,710,730 nm.

Similarly, the separable scatterplots in the discriminative range of green and red wavebands (Figure 6) confirmed the possibility of weed species classification in Mayville research site. In general, the differences in the spectral responses between crop and weed species in visible blue, green and red wavebands can be attributed to variations caused by the differences in the chlorophyll content of the plants.

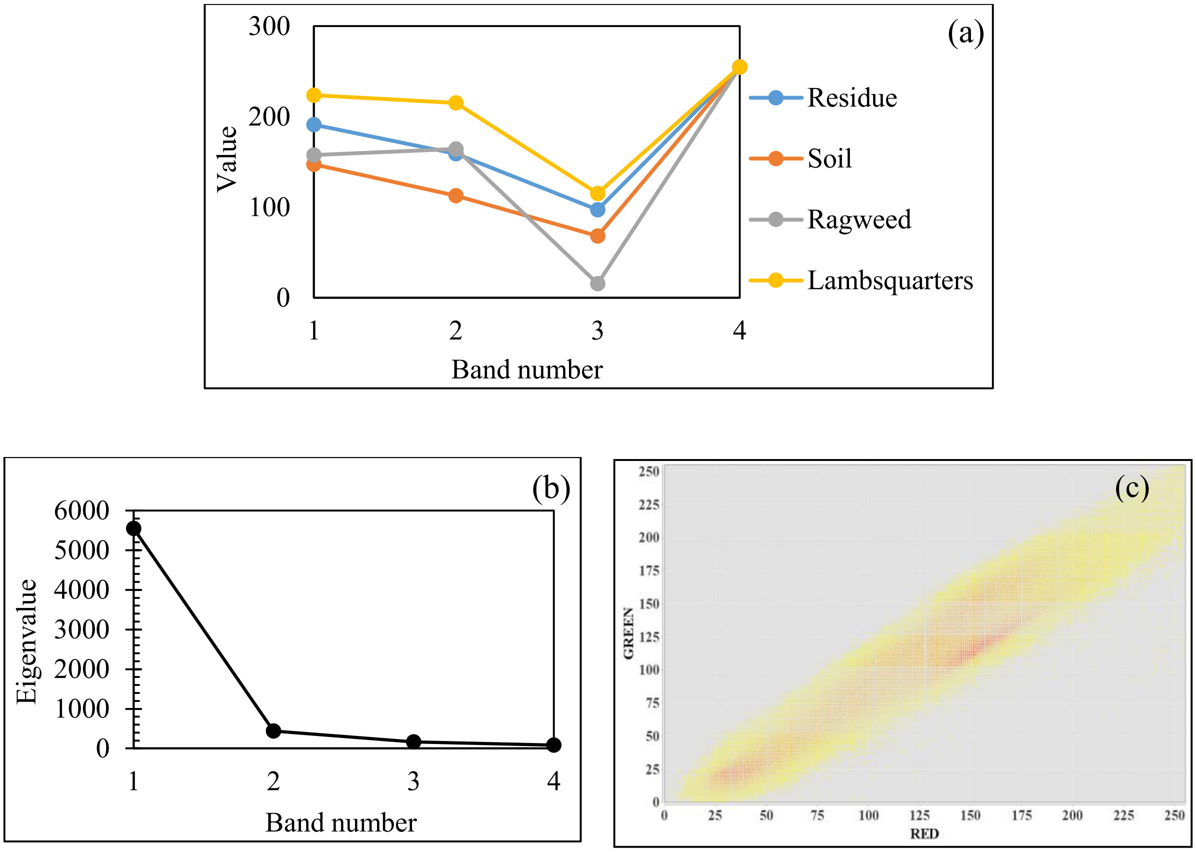

Figure 6. Assessment of feasibility of field components classification in Mayville study site: a) Spectral signature, b) PC plane, and c) Scatterplot of spectral reflectance. Band number 1 through 4 are RGB, 670,710,730 nm.

3.2. Crop and Weed Species Classification Accuracy

At high spatial resolution, it is possible to distinguish the different leaf shapes and textures for the different target classes. The accuracy of classifying the target classes (main crop, weed species, soil and residue) in the experimental fields using OBIA and PBIA classification algorithms is listed in Table 4. All six classification algorithms resulted in lower the overall accuracies and Kappa coefficients under the pixel-based analysis, compared to object-based analysis. Lower accuracies of PBIA methods indicate that soil background, residue, and shadow in mixed pixel may cause variabilities that reduce the classification accuracy.

The SVM method resulted in the highest classification accuracy of 98-99%, and kappa coefficient of 0.99-1 under object-based classification. In OBIA method, all classification methods except MD algorithm exhibited high classification accuracies with overall accuracies greater than

86% and Kappa coefficients greater than 0.77. A supervised classification strategy is considered acceptable if the overall classification accuracy higher than 85%, and Kappa coefficient higher than 0.75 (Castillejo-González et al., 2014). Therefore, the OBIA classification with P, ML, SVM, SAM, DT methods exhibited accuracies higher than the minimum acceptable levels (Table 4). However, the MD classifier with the overall accuracy of 74% and Kappa coefficient of 0.6 didn't reach the commonly accepted requirements. This observation might be attributed to the disability of simple MD analysis to detect small variations in spectral reflectivity (Morozova, Elizarova, & Pleteneva, 2013).

Table 4. Classification accuracy of weed species using different supervised classification algorithms at Carrington (S1) and Mayville (S2) study sites.

Supervised classification method	Pixel-based				Object-based			
	OA[a] (%)		K[b]		OA (%)		K	
	S_1[c]	S_2[d]	S_1	S_2	S_1	S_2	S_1	S_2
Parallelepiped (P)	78	86	0.69	0.78	85	90	0.77	0.82
Maximum Likelihood (ML)	83	87	0.65	0.86	91	97	0.86	0.94
Mahalanobis Distance (MD)	67	85	0.58	0.85	74	95	0.6	0.93
Support Vector Machine (SVM)	92	93	0.87	0.9	99	98	1	0.96
Spectral Angle Mapper (SAM)	87	85	0.8	0.83	92	91	0.86	0.81
Decision Tree (DT)	88	89	0.87	0.92	94	97	0.91	0.95

OA[a]: overall accuracy, K[b]: Kappa coefficient

In PBIA method, the most comparable classification results were observed with SVM method. The SVM classifier exhibited the overall accuracy and Kappa coefficient of 92-93% and 0.87-0.9, respectively. While, MD classification algorithm resulted in the lowest overall accuracy of 67% and Kappa value 0.58 for the Carrington location.

The distribution of soybean crops, waterhemp and kochia weed species, soil and the other field components in Carrington field in multispectral image were analyzed using all the classification algorithms evaluated with the PBIA and OBIA methods (Figure 7.).

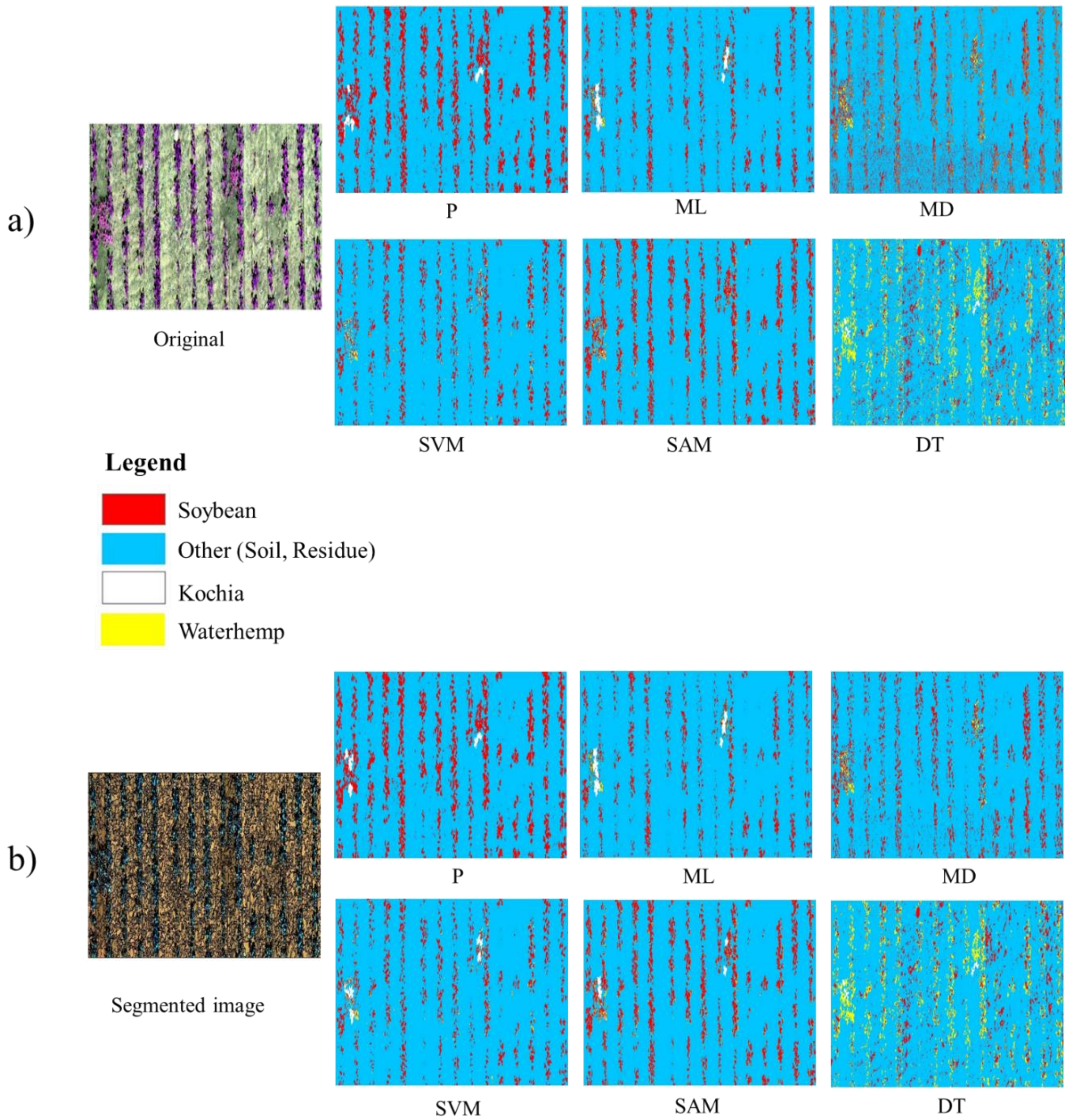

Figure 7. Comparison of a) PBIA and b) OBIA classification algorithms in Carrington study site.

Similarly, the results of classified images for two weed species including lambsquarters and ragweed, bare soil and residue in Mayville research site using all the classification algorithms through PBIA and OBIA methods are illustrated in Figure 8.

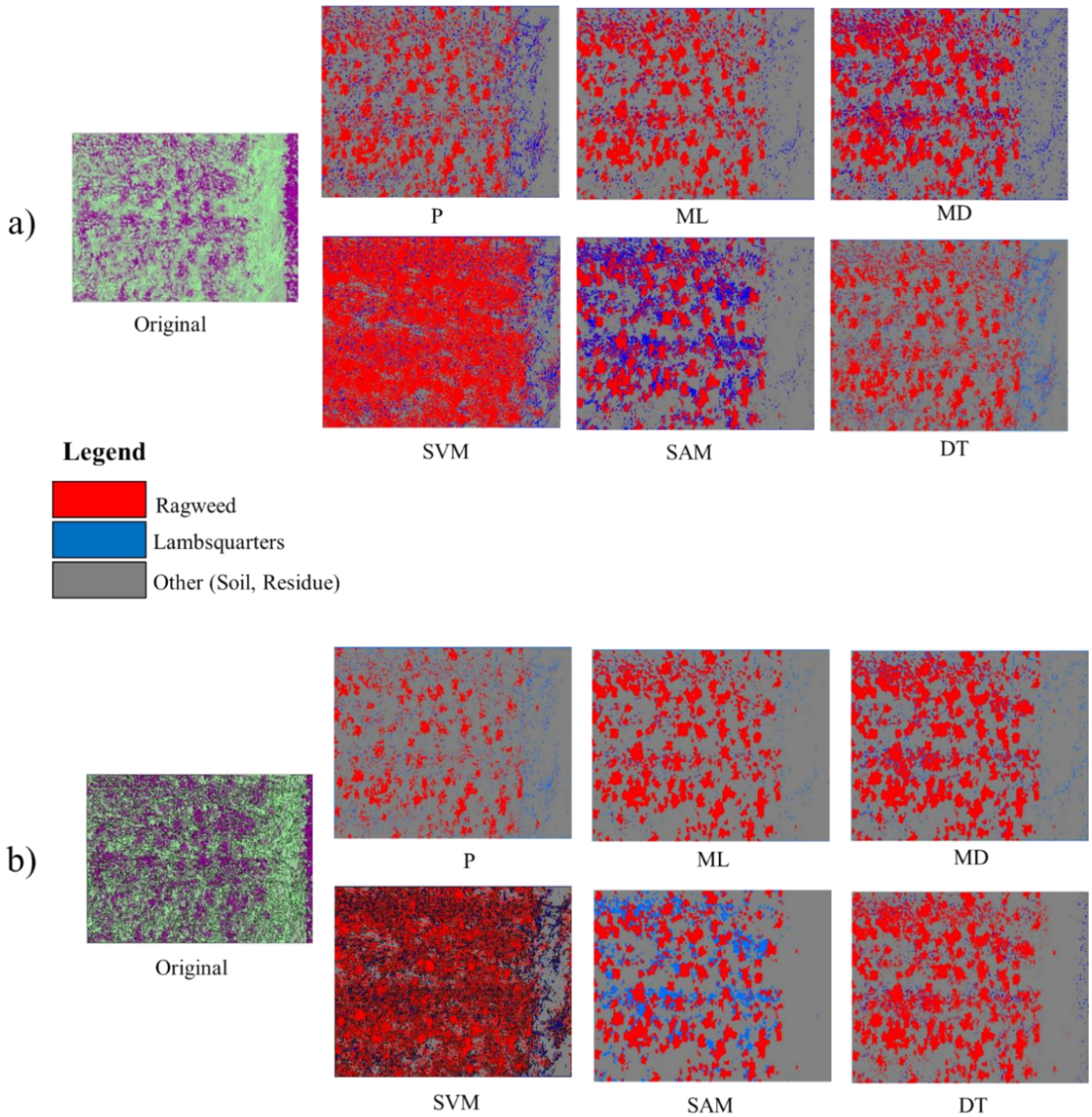

Figure 8. Comparison of a) pixel- and b) object-based classification algorithms in Mayville study site.

All classifiers under PBIA and OBIA exhibited higher overall accuracy in Mayville field in comparison to Carrington site. This observation was related to the reduction of crop-plant detection ability in the multispectral images as a classified object. Furthermore, the relatively higher phenological difference between lambsquarters and ragweeds in Mayville field than soybean and weed species (waterhemp and kochia) in Carrington might be another factor in enhancing weed detection accuracy in Mayville. This fact confirmed that the spectral reflectance similarity between plant species in early growth season is a limiting factor in PBIA. However, OBIA methods by segmenting the images into groups of adjacent pixels with homogenous spectral values displayed higher detection accuracy for weed species by reducing some of the pixel to pixel variability.

Although all the classifiers worked with the same data, SVM and DT algorithms required longer processing times. More complicated computational processing made SVM and DT more sensitive and accurate in comparison to MD, ML and p algorithms with a fast and facile procedure for weed species classification early after plant germination. The two simple MD and ML algorithms yielded very accurate results in Mayville site where there were two weed species for discriminating, while their classification accuracy was lower in Carrington site in which soybean was added to classified objects.

Clear difference was observed between the OBIA and PBIA classifications in all supervised classification methods evaluated in this study. The integration of segmented objects in the studied classifiers resulted in an increase in overall accuracy in OBIA classification methods. The ML classifier exhibited 10% higher overall accuracy through OBIA classification platform in comparison with PBIA method in Carrington site study. While, the least growth in overall accuracy was seen in P with 4% increase in OBIA with segmentation in Mayville site. Similar observation was reported by López Granados (2011). On one hand, a high spatial resolution of the remote images is required for weed detection, however, the higher spatial resolution is penalised with lower spectral resolutions limited to the visible and NIR spectral regions. The similar morphology between plant species in early growing season cause low spectral differentiation between weed species and main crop. Therefore, the combination of spectral and spatial characteristics produced a significant improvement over the precision obtained in the object-based classifications. Although, OBIA was more time and effort- intensive due to the initial segmentation process for which more expert knowledge and more specialised software were required, the overall classification accuracy exceeded the performance achieved using PBIA algorithm. Therefore, in this study the object-based had great potential and advantages for weed species detection in early growth stage.

3.3. Glyphosate-Resistant and Glyphosate-Susceptible Weed Accuracy

The plant canopy temperature extracted from the thermal images indicated that the temperature of susceptible weeds increased after glyphosate application. The resistant weeds in

Carrington and Mayville exhibited much lower canopy temperature in comparison with the susceptible weeds for all three-weed species (Table 5).

Table 5. Mean values of canopy temperatures in Carrington (S1) and Mayville (S2) study sites.

Study site	Weed species	Canopy temperature (°C)	
		Resistant weeds	Susceptible weeds
S1	Kochia	26.12 ±0.11	27.95± 0.25
	Waterhemp	27± 0.18	28.85±0.19
S2	Ragweed	28.04 ±0.21	29.96±0.33

The temperature variance in weed species with different level of susceptibility is a result of physiological mechanism involved in the photosynthesis process. The application of herbicide leads to a poor photosynthetic efficiency accompanied by a significant loss of light energy as heat in the susceptible plants (Gomes et al., 2017). The IR Flash window which illustrates the colorized thermal image over weed plants is shown in Figure 9 and 10. The IR256 color lookup ramp was used for temperature variance visualization, in which the area with lower temperatures were displayed in blue and the hottest canopies were presented in red and followed by green. Glyphosate-resistant waterhemp weeds are shown by green color (27.18 °C) in the Carrington experimental field in comparison with susceptible weeds which were shown in red (28.99°C). In Mayville, the resistant-ragweed plants are revealed by the blue color (28.14 °C) in IR Flash window while susceptible are displaced in green (30.06 °C).

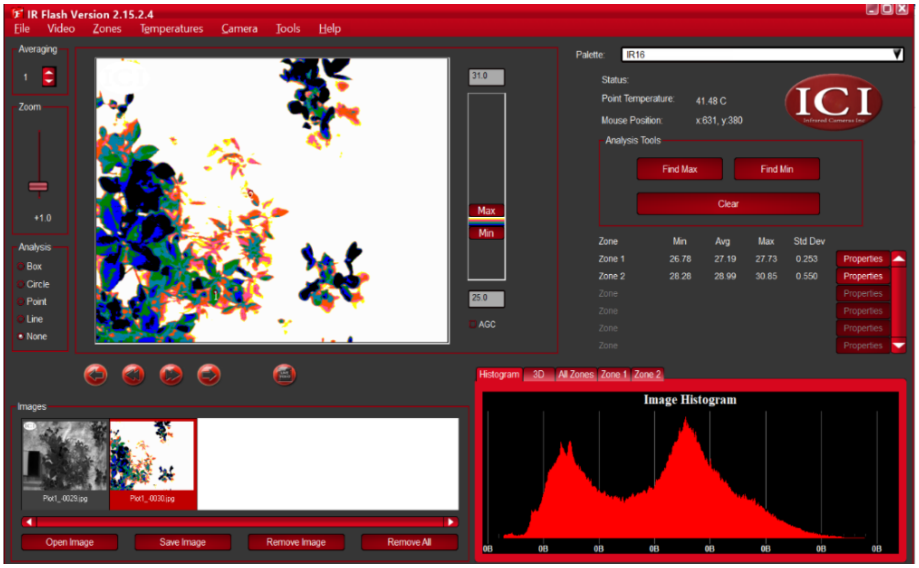

Figure 9. A thermal image of the waterhemp plants (Carrington study site) in IR Flash software. Zone 1(green) indicates Resistant waterhemp. And Zone 2 (red) indicates susceptible waterhemp. The average temperature for the various zones can be seen on the right-hand panel.

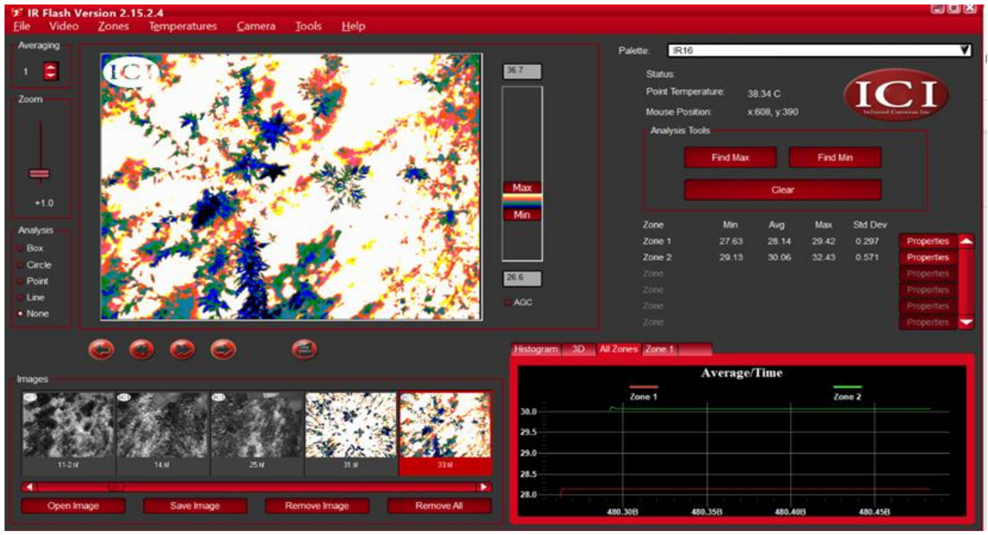

Figure 10. The thermal image of the ragweed plants (Mayville study site) in IR Flash software. Zone 1 (blue) # Resistant ragweed. Zone 2 (green) # susceptible ragweed. The average temperature for the various zones can be seen on the right-hand panel.

The results were compared with the ground truth data after observing the death symptoms in susceptible weeds. (Table 6).

Table 6. Summary of glyphosate-resistant weed classification accuracy at Carrington (S1) and Mayville (S2) study sites.

Study site	Weed species	Weed No.		Resistant weed classification accuracy			
		Resistant	Susceptible	Accuracy %	Sensitivity	Specificity	Precision
S1	Kochia	25	36	88	0.83	0.92	0.87
	Waterhemp	27	41	93	0.91	0.95	0.90
S2	Ragweed	56	21	92	0.89	0.95	0.88

The overall accuracy was 88%, 93% and 92% for kochia and waterhemp in Carrington site, and ragweed in Mayville research field, respectively. The high accuracy for all three-weed species in two different locations indicated that plant canopy temperature can be a reliable discriminative feature for identifying glyphosate-resistant weeds early after spraying, and even before observing stress symptom on plants. The false positive and negative errors were interpreted by the fact that weeds varied in their level of susceptibility to glyphosate. In fact, there were some actual resistant weeds while their temperature raised early after spraying. However, they were survived after 15 days when the drying symptom was observed on susceptible weeds.

4. Conclusions

In this field study, the potential application of supervised classification methods and canopy temperature in weed species and glyphosate-resistant weed detection were evaluated. Supervised object-based and pixel-based image analysis strategies were employed to assess six different classification methods including Parallelepipeds (P), Mahalanobis Distance (MD), Maximum Likelihood (ML), Spectral Angle Mapper (SAM), Support Vector Machine (SVM) and Decision Tree (DT). The object-based algorithms developed with mosaicked imagery effectively classified weed species with the overall accuracy and Kappa coefficient values greater than 86% and 0.77, respectively. However, the performance of pixel-based classification methods was limited in early growth stages due to the high similarity between weed species. Overall, the canopy temperature variation within the crop species provided a novel approach for identifying glyphosate-resistant weeds with the accuracy of 88%, 93% and 92.6% for kochia, waterhemp and ragweed. The results of this study can be used in support of SSWM to inhibit the distribution of resistant weeds across the fields.

Acknowledgment

We thank Dr. Zollinger and Dr. Ostlie from NDSU for their help with the field experiment. The authors would like to thank the North Dakota Agricultural Experiment Station, North Dakota Soybean Council, and the North Dakota Department of Commerce (grant number FAR0024073) for providing grant support to conduct this research.

REFERENCES

Benbrook, C. M. (2018). Why Regulators Lost Track and Control of Pesticide Risks: Lessons From the Case of Glyphosate-Based Herbicides and Genetically Engineered-Crop Technology. *Current environmental health reports, 5*(3), 387-395.

Castillejo-González, I. L., Pena-Barragán, J. M., Jurado-Expósito, M., Mesas-Carrascosa, F. J., & López-Granados, F. (2014). Evaluation of pixel-and object-based approaches for mapping wild oat (Avena sterilis) weed patches in wheat fields using QuickBird imagery for site-specific management. *European Journal of Agronomy, 59*, 57-66.

Che'Ya, N. N. (2016). Site-Specific Weed Management Using Remote Sensing.

Gålfalk, M., Karlson, M., Crill, P., Bousquet, P., & Bastviken, D. (2018). A simple approach for efficient collection of field reference data for calibrating remote sensing mapping of northern wetlands. *Biogeosciences, 15*(5), 1549.

Garcia-Ruiz, F., Sankaran, S., Maja, J. M., Lee, W. S., Rasmussen, J., & Ehsani, R. (2013). Comparison of two aerial imaging platforms for identification of Huanglongbing-infected citrus trees. *Computers and Electronics in Agriculture, 91*, 106-115.

Gomes, M. P., Manac'h, L., Sarah, G., Hénault-Ethier, L., Labrecque, M., Lucotte, M., & Juneau, P. (2017). Glyphosate-dependent inhibition of photosynthesis in willow. *Frontiers in plant science, 8*, 207.

Hunt, E. R., Hively, W. D., Fujikawa, S. J., Linden, D. S., Daughtry, C. S., & McCarty, G. W. (2010). Acquisition of NIR-green-blue digital photographs from unmanned aircraft for crop monitoring. *Remote Sensing, 2*(1), 290-305.

Kunz, C., Weber, J. F., Peteinatos, G. G., Sökefeld, M., & Gerhards, R. (2018). Camera steered mechanical weed control in sugar beet, maize and soybean. *Precision Agriculture, 19*(4), 708-720.

Lambert, J., Hicks, H., Childs, D., & Freckleton, R. (2018). Evaluating the potential of Unmanned Aerial Systems for mapping weeds at field scales: a case study with Alopecurus myosuroides. *Weed research, 58*(1), 35-45.

Liu, T., & Abd-Elrahman, A. (2018). Multi-view object-based classification of wetland land covers using unmanned aircraft system images. *Remote Sensing of Environment, 216*, 122-138.

Morozova, M., Elizarova, T., & Pleteneva, T. (2013). Discriminant analysis and Mahalanobis distance (NIR diffuse reflectance spectra) in the assessment of drug's batch-to-batch dispersion and quality threshold establishment. *European Scientific Journal, ESJ, 9*(27).

Pandya, R., & Pandya, J. (2015). C5. 0 algorithm to improved decision tree with feature selection and reduced error pruning. *International Journal of Computer Applications, 117*(16), 18-21.

Pena, J. M., Torres-Sánchez, J., de Castro, A. I., Kelly, M., & López-Granados, F. (2013). Weed mapping in early-season maize fields using object-based analysis of unmanned aerial vehicle (UAV) images. *PloS one, 8*(10), e77151.

Pérez-Ortiz, M., Peña, J., Gutiérrez, P. A., Torres-Sánchez, J., Hervás-Martínez, C., & López-Granados, F. (2015). A semi-supervised system for weed mapping in sunflower crops using unmanned aerial vehicles and a crop row detection method. *Applied Soft Computing, 37*, 533-544.

Pflanz, M., Nordmeyer, H., & Schirrmann, M. (2018). Weed Mapping with UAS Imagery and a Bag of Visual Words Based Image Classifier. *Remote Sensing, 10*(10), 1530.

Schütte, G., Eckerstorfer, M., Rastelli, V., Reichenbecher, W., Restrepo-Vassalli, S., Ruohonen-Lehto, M., . . . Mertens, M. (2017). Herbicide resistance and biodiversity: agronomic and environmental aspects of genetically modified herbicide-resistant plants. *Environmental Sciences Europe, 29*(1), 5.

Sosnowski, T., Bieszczad, G., Madura, H., & Kastek, M. (2018). *Thermovision system for flying objects detection.* Paper presented at the 2018 Baltic URSI Symposium (URSI).

Stephens, D., & Diesing, M. (2014). A comparison of supervised classification methods for the prediction of substrate type using multibeam acoustic and legacy grain-size data. *PloS one, 9*(4), e93950.

Voyant, C., Notton, G., Kalogirou, S., Nivet, M.-L., Paoli, C., Motte, F., & Fouilloy, A. (2017). Machine learning methods for solar radiation forecasting: A review. *Renewable Energy, 105*, 569-582.

Zhang, C., Filella, I., Garbulsky, M. F., & Peñuelas, J. (2016). Affecting factors and recent improvements of the photochemical reflectance index (PRI) for remotely sensing foliar, canopy and ecosystemic radiation-use efficiencies. *Remote Sensing, 8*(9), 677.